

A STUDY OF THE X-RAY EMISSION FROM  
THE PLASMA FOCUS

*by*

GRAHAM WHITELOW RANKIN

B.Sc., The University of British Columbia, 1972

A THESIS SUBMITTED IN PARTIAL FULFILMENT OF  
THE REQUIREMENTS FOR THE DEGREE OF  
MASTER OF SCIENCE

in the Department  
of  
PHYSICS

We accept this thesis as conforming to the  
required standard

THE UNIVERSITY OF BRITISH COLUMBIA

December, 1975

In presenting this thesis in partial fulfilment of the requirements for an advanced degree at the University of British Columbia, I agree that the Library shall make it freely available for reference and study.

I further agree that permission for extensive copying of this thesis for scholarly purposes may be granted by the Head of my Department or by his representatives. It is understood that copying or publication of this thesis for financial gain shall not be allowed without my written permission.

Department of physics

The University of British Columbia  
2075 Wesbrook Place  
Vancouver, Canada  
V6T 1W5

Date Dec. 1, 1975

## ABSTRACT

The X-ray emission from a plasma focus has been studied using time integrated and streak photography. The plasma focus, a small volume of very dense and hot plasma was created in a coaxial plasma gun driven by a fast current pulse of period  $T \approx 2 \mu\text{sec}$  which was produced by discharging a condensor bank of  $V = 12\text{-}15 \text{ kV}$ , and  $C = 84 \mu\text{f}$ .

Measurements have shown that a diffuse X-ray emitting plasma column is formed in the 'early' pinch stage, which extends a few centimeters in the axial direction, has expansion velocities of between  $2\text{-}6 \times 10^7 \text{ cm/sec}$ . and lasts for 30-60 nsec.

In the following 10-30 nsec. X-ray emission occurs from small plasma regions which have little or no axial velocity. The distance between these "hot" spots are of the order of half a centimeter.

These measurements and observations of the X-ray emitting regions are consistent with results obtained by Peacock and Mather. By comparing their results with those of this experiment it is concluded that the appearance of the isolated X-ray sources is associated with the  $m = 0$  instability.

# TABLE OF CONTENTS

	<u>Page</u>
ABSTRACT . . . . .	ii
LIST OF FIGURES. . . . .	v
ACKNOWLEDGMENTS. . . . .	vi
 <u>Chapter</u>	
1 INTRODUCTION . . . . .	1
1.1 The Plasma Focus . . . . .	1
1.2 Previous Work on the Plasma Focus. . . . .	3
1.3 Uniqueness of the Experiment . . . . .	4
2 APPARATUS. . . . .	6
2.1 The Focus. . . . .	6
2.2 The Spark Gap. . . . .	9
2.3 X-ray Imaging. . . . .	11
2.4 Timing . . . . .	15
3 OBSERVATIONS AND RESULTS . . . . .	18
3.1 Image Magnification. . . . .	18
3.2 Spacial Resolution . . . . .	19
3.3 Temporal Resolution. . . . .	19
3.4 X-ray Photographs. . . . .	19

<u>Chapter</u>		<u>Page</u>
4	DISCUSSION OF RESULTS. . . . .	23
5	CONCLUSIONS. . . . .	28
	REFERENCES . . . . .	29

## LIST OF FIGURES

<u>Figure</u>		<u>Page</u>
1	Experimental arrangement. . . . .	7
2	Electrode assembly. . . . .	8
3	Spark gap electrodes. . . . .	10
4	Electrical circuit of the plasma focus. . . . .	12
5	Illustration of Optical arrangement . . . . .	13
6	Pinhole . . . . .	14
7	Electro-optical X-ray camera. . . . .	16
8	Triggering arrangement. . . . .	17
9	X-ray photographs and an oscillogram of the focusing event . . . . .	21
10	Schematic for proposed sequence of events. . . . .	27

## ACKNOWLEDGMENTS

The idea of using streak photography for analyzing the dense pinch stage of the plasma focus is that of Dr. J. Meyer.

I would like to acknowledge the building of the plasma focus apparatus by Jack Burnett.

To Dough Sieberg and Allen Cheuck, I wish to express my appreciation for their technical assistance.

Many thanks to the members of the U.B.C. plasma physics group for their helpful discussions.

This work was supported by a grant from the Atomic Energy Control Board of Canada.

## Chapter 1

### INTRODUCTION

#### 1.1 The Plasma Focus

The plasma focus is a device consisting of coaxial electrodes inside a vessel containing a mixture of gases at a pressure of less than several torr.

The formation of the dense plasma focus beyond the end of the coaxial electrode geometry was first observed and studied by the Russian, T.I. Flippova in the 1960's.

Over the years studies of the plasma focus have concentrated on the initial electrical breakdown between the electrodes, the dynamics of the rundown of the current sheath, and the final dense focus stage of the plasma focus, with recent interest being on the latter and more specifically on the neutron production which results if a  $D_2$  gas is used in the discharge vessel.

A high voltage (in this expt. 12-15 kV) from the capacitor bank is applied between the inner and outer electrodes of the discharge vessel. This produces a breakdown in the region at the back of the electrodes near a Lucite



insulator (see Fig. 1). Current then flows from the centre electrode back along the insulator to the back plate producing a "waterfall" flow over the insulator surface. Studies have shown [1] that during the early stages of current build-up there is a complex filamentary light pattern produced at the back plate. The  $j_z \times B_\theta$ , inverse pinch force next drives the current outward towards the outer electrode. At this time the filamentary pattern of the current blends to form a uniform axisymmetric discharge.

Because  $j_r$  and  $B_\theta$  decrease with radius the force ( $j_r \times B_\theta$ ) is greater nearer the inner electrode than at the outer electrode and so the current sheath has a cant. Photographs by Mather [2] have shown this appearance of the sheath.

The current sheath as it moves down between the copper electrodes accumulates gas in front of it. This effect called snowploughing has led to several models describing the physics of the current sheath [3]. The maximum average sheath velocity in the annulus has been recorded to have an upper limit of  $1.5 \times 10^7$  cm/sec [4].

When the current sheath arrives at the end of the electrodes it overshoots and experiences a fast ( $1-4 \times 10^7$  cm/sec) [5] radial collapse towards the axis as a result of the strong radial pinch force,  $j_z \times B_\theta$ . To maximize this pinch force one chooses the gas mixture, and the voltage such that the peak of the current pulse occurs at the time of

radial collapse. In addition the peak of the current pulse is determined by the inductance of the voltage supply network. Any reduction in the inductance, for example, by using several low inductance cables to deliver the current from the capacitor bank to the discharge vessel will result in achieving a greater pinch force.

The dense plasma formed as a result of the pinch has been observed to have electron densities of order  $10^{19}$   $\text{cm}^{-3}$  and temperature of several keV.

## 1.2 Previous Work on the Plasma Focus

Measurements of densities have been done by observing the shape of the emission spectrum and the absolute radiation flux in the soft X-ray region [8]. Shadowgraphs and Schlieren photographs have been used to determine the spacial and temporal development of the dense plasma [12], and interferometric measurements have been used to obtain the electron density [4]. The fitting of data to both X-ray emission and neutron yields (assuming a thermonuclear plasma) have given plasma densities of the order of  $10^{19}$   $\text{cm}^{-3}$  [4].

Electron temperatures (for deuterium) of approximately .70 keV have been observed by laser scattering [7]. In addition, it has been observed that in a deuterium plasma the total neutron emission per discharge requires an ion temperature of several keV (assuming a thermonuclear plasma

[6]). The assumption of thermal neutron production is not clearly valid since there is evidence for a nonthermonuclear production in a deuterium plasma focus [9].

Due to the high temperatures reached in the plasma focus most of the radiation is in the X-ray region. These X-rays are due to Bremsstrahlung and line radiation. This thesis devotes its main interest to the investigation of the X-ray emission features of the dense focus stage. The focus at U.B.C. does not produce neutrons and as such is primarily an X-ray emitting plasma.

### 1.3 Uniqueness of the Experiment

What is unique about this experiment performed at the U.B.C. plasma physics lab is that it is the first experiment to take streak photographs of the X-ray emissions during the focus stage of the pinch. Other experiments which have investigated the X-ray emission features of the focus have included the recording of X-ray emissions by the use of X-ray pinhole cameras with various absorbers to obtain time integrated photographs and thus information about the energies of the X-rays emitted, in addition to correlation of framing pictures (in the visible region) with X-ray monitored pulses.

Most of the theoretical work done on the plasma focus so far has been to explain the observations of the neutron flux that originates from a deuterium focus. To

explain the anisotropic distribution of neutron fluxes and neutron energy spectra various models have been proposed, as for example the beam target model, and other models, which assume thermal and thermonuclear processes occurring within the focus.

Observations and possible mechanisms of X-ray emission features have been studied by such noted experimentalists in this field as Peacock and Mather and to a lesser extent Bostick. Their observations and proposed mechanisms in conjunction with what has been observed at the U.B.C. plasma focus is discussed and summarized in the conclusion of this thesis.

In summary it was the aim of this experiment to measure velocities and lifetimes of the X-ray emitting plasma and to compare the X-ray time integrated photographs with those obtained by other experimentalists, and to fit and compare the results obtained with existing models so that a possible mechanism for X-ray production could be formulated.

The experiment was a success in that the spacial and temporal features of the X-rays using nsec. streak, and time integrated photography were recorded and analyzed. As a result a possible mechanism for X-ray production could be formulated.

## Chapter 2

### APPARATUS

#### 2.1 The Focus

The experimental arrangement is shown in Fig. 1. The plasma focus investigated in this experiment consists basically of two coaxial cylindrical copper electrodes of approximately 25 cm in length. The inner electrode cylinder of positive polarity has an outer diameter of 5 cm and an inner diameter of 2.5 cm. The cathode is a perforated copper cylinder of 10 cm diameter. The outer cylinder is soldered onto a brass disk with a concentric hole of 6 cm diameter. The hole allows the coaxial assembly consisting of the anode, and a cylindrical Pyrex insulator (5 cm inner diameter and 5 cm length), which is fitted over the anode, to be mounted inside the outer cylinder (see Fig. 2).

The glass sleeve and a plexiglass disk prevent premature electrical breakdown between the opposite polarity electrodes. In addition the glass sleeve allows the initial formation of an inverse pinch following breakdown to occur between the anode at the sleeve end and the inside of the copper cathode cylinder.

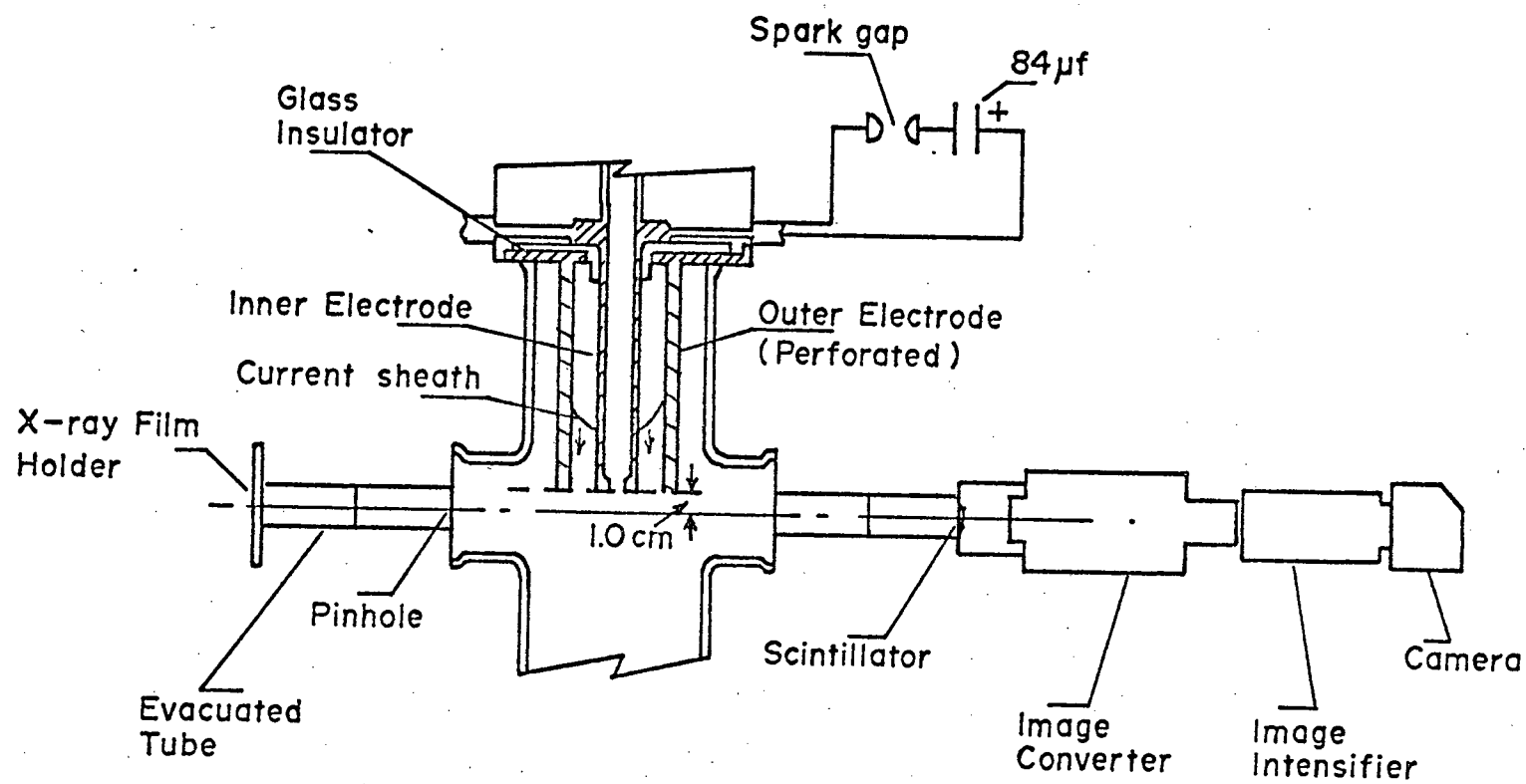


Figure 1. Experimental arrangement.

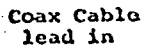


Figure 2. Electrode assembly.

The entire electrode assembly is fitted inside a Pyrex vessel which is evacuated and filled with a gas mixture of Hydrogen and Argon (approximately 10% Argon by pressure) to a pressure of between .5 to .8 Torr.

The electrode assembly is held in position in the Pyrex vessel by a brass plate. The brass plate (or cable header) also provides an electrical connection between the coaxial cables coming from the capacitor bank to the inner and outer cylindrical copper electrodes (located inside the Pyrex vessel).

The power required to produce the current sheath is provided by a bank of six, 14 uf capacitors charged to a voltage between 12 and 15 kV. This energy is delivered by 30 coaxial cables (five cables for each capacitor) which are all connected to the cable header.

## 2.2 The Spark Gap

Each capacitor has a spark gap. All spark gaps are triggered at the same time by a pulse produced by firing an auxiliary spark gap. Inside the spark can, which houses the spark gap, are four electrodes. Fig. 3 depicts the four electrodes. One electrode (#2 in the diagram) is connected to the high voltage terminal of the capacitor and another (#1) is electrically connected (via the cable header) to the inner positive cylindrical electrode.



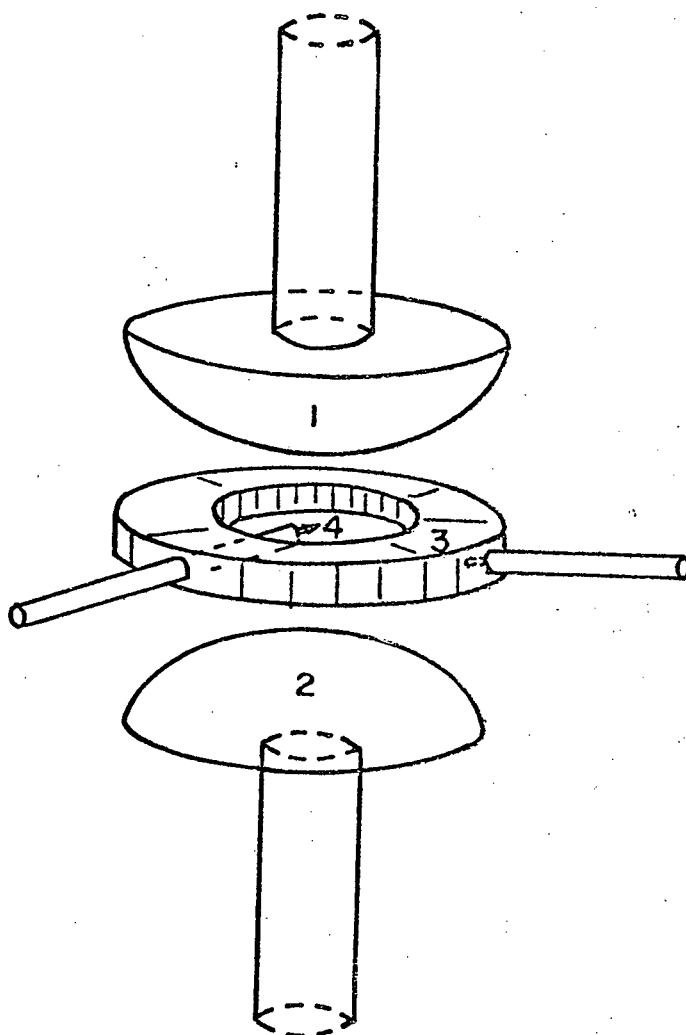


Figure 3. Spark gap electrodes.

Two other electrodes (#3 and #4) are located between the above mentioned electrodes. A high voltage pulse (produced by the auxiliary spark gap) is applied between the outer disk shaped electrode (#3) and the fine point of a tungsten wire (electrode #4), so that a spark is produced between them. This spark produces a U.V. flash which in turn ionizes the air and causes a current to start flowing between electrodes #1 and #2. The resulting plasma short circuits electrodes #1 and #2 and thereby discharges the capacitor.

This electrical arrangement of the spark gap ensures a fast and jitter-free breakdown of the capacitor bank. This is important since simultaneous arrival of the voltage pulses at the cable header is important for the formation of a good focus. See Fig. 4 for the detailed electrical layout.

### 2.3 X-ray Imaging

Time integrated and streaked X-ray photographs were taken simultaneously of the same plasma focus event. The imaging was accomplished by using a pinhole X-ray camera.

Located at right angles to the electrode axis (and approximately 17 cm from the focus) are pinholes of .5 mm (one on each side) with a 1 mil Be foil window (see Figs. 5 and 6). The pinhole diameter is of the order of a thousand Fresnel zones wide. The X-rays passing through the pinholes

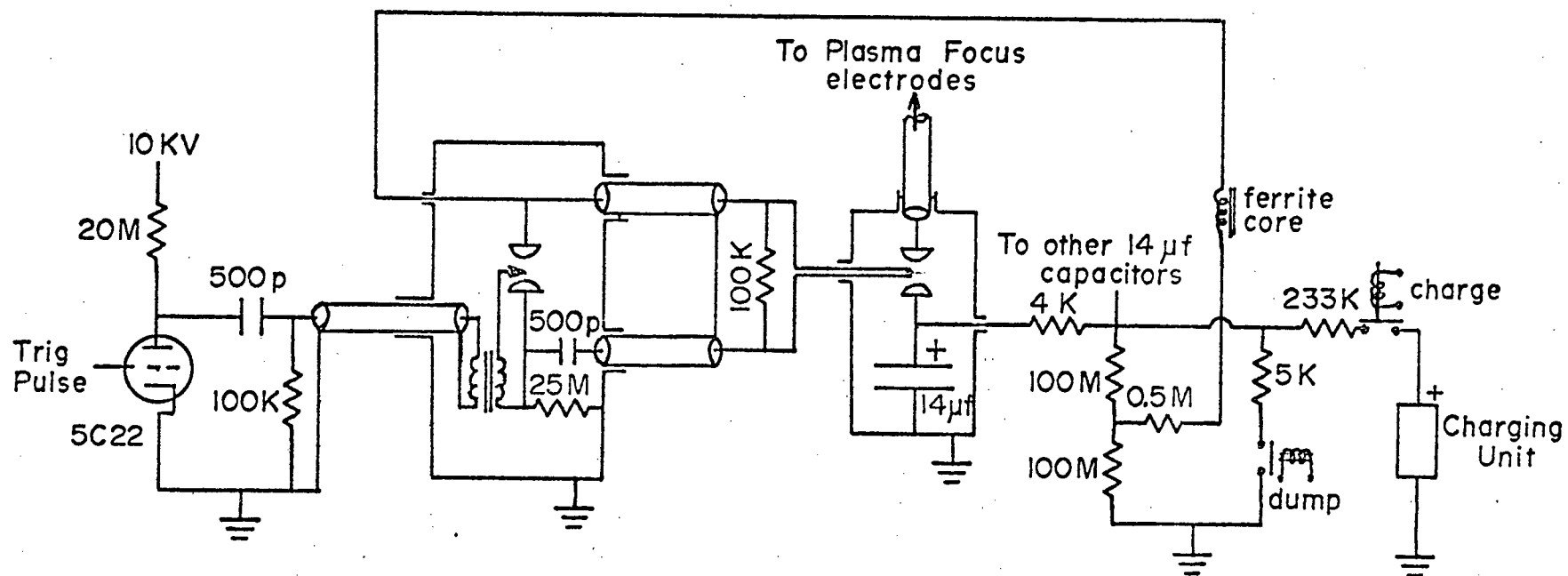


Figure 4. Electrical circuit of the plasma focus.

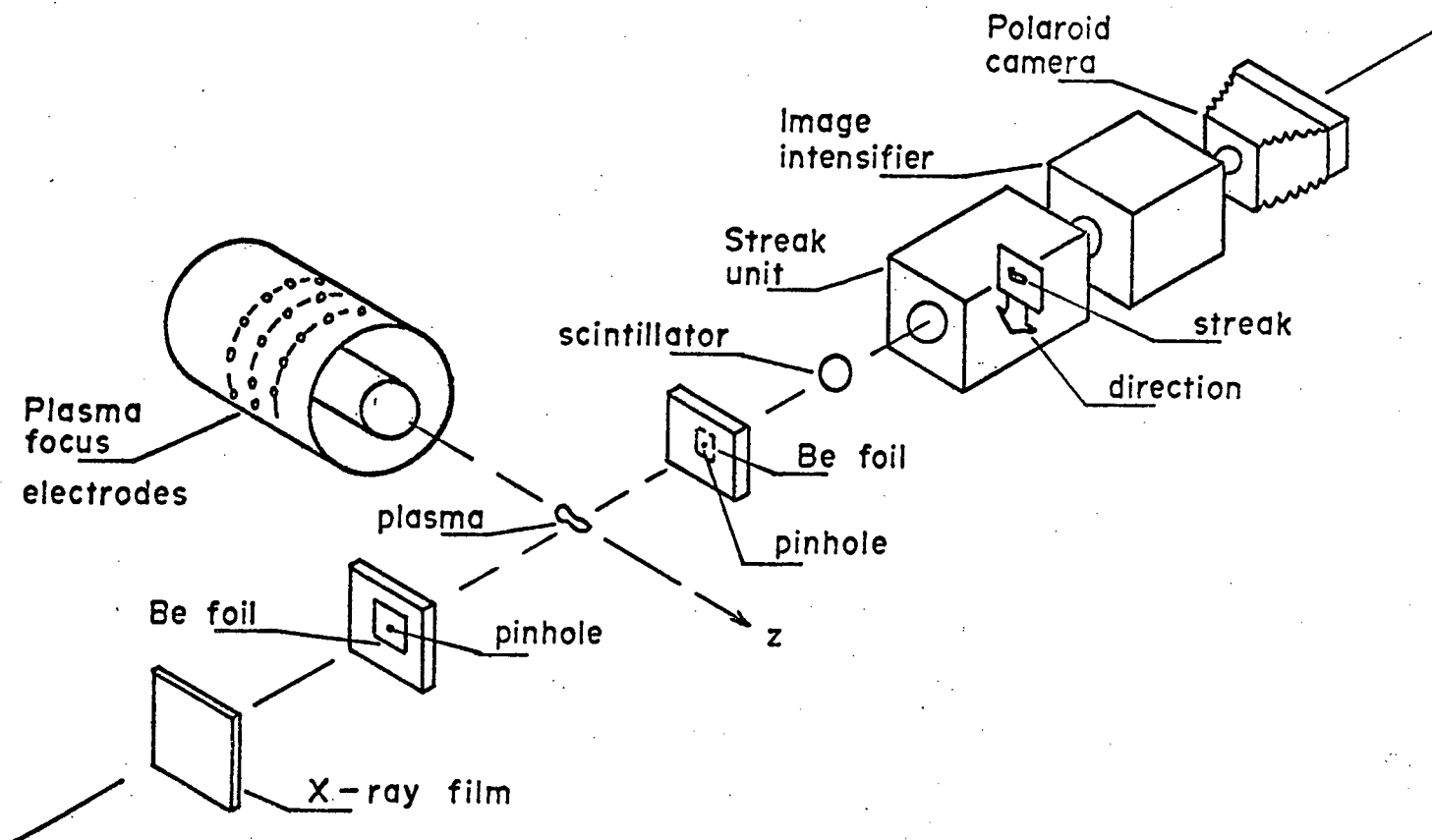


Figure 5. Illustration of optical arrangement.

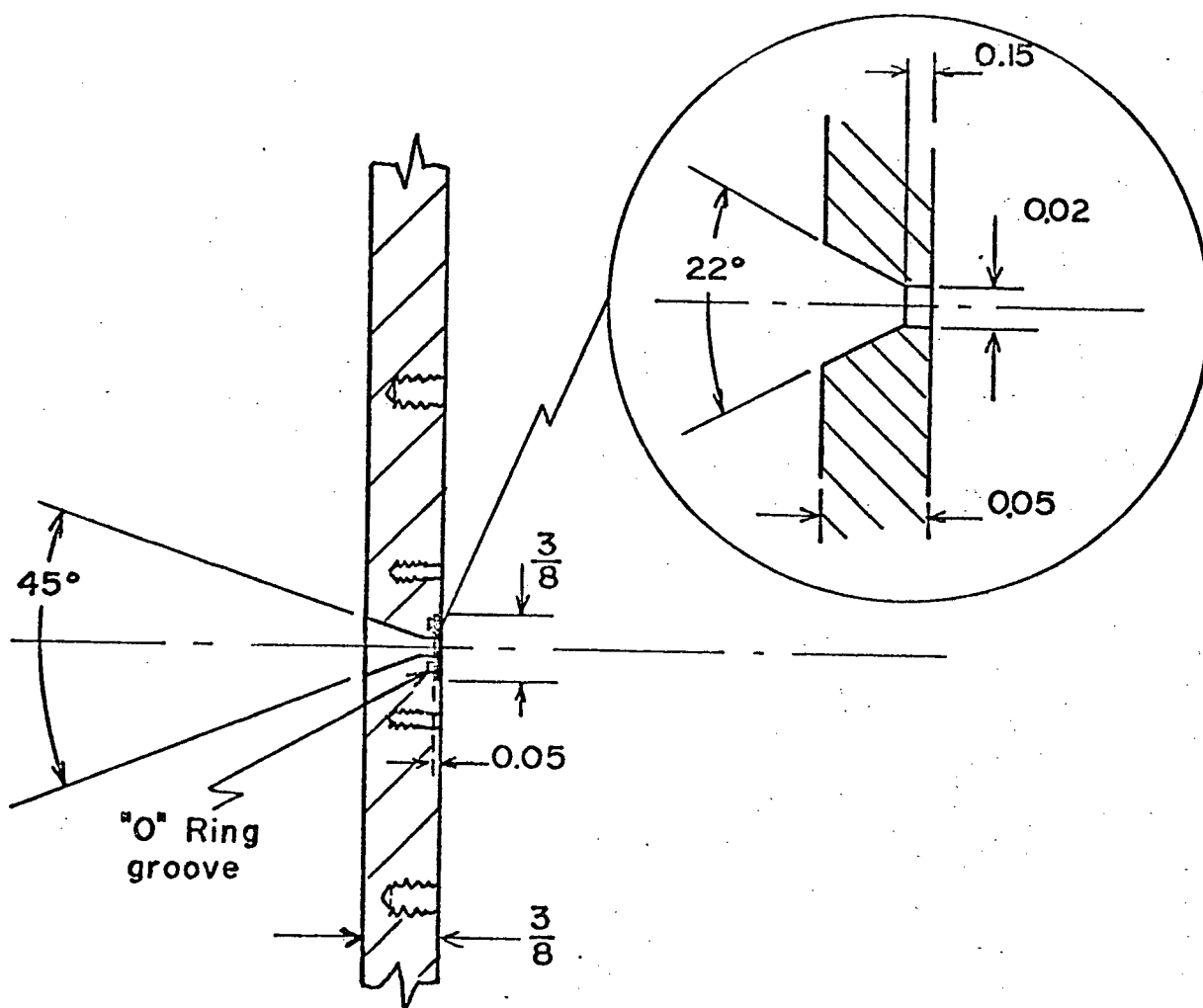


Figure 6. Pinhole.

travel down an evacuated hollow tube (approximately 17 cm in length) until they hit in one case X-ray recording film or in the other a thin scintillator (1.5 mm) producing an image in visible light. This image is time resolved by a TRW Image Converter Camera. The streaked image is then passed through an image intensifier (RCA 8606) before finally being recorded by a camera onto 10,000 A.S.A. polaroid film (Fig. 7).

#### 2.4 Timing

The timing required to take the X-ray streak pictures was achieved by placing a light pipe near the end and above the outer perforated electrode. As the luminous front of the current sheath passed down between the electrodes the light radiated from it was picked up by the light pipe (see Fig. 8) and then sent to a photomultiplier which in turn triggered the delay generator which sent a pulse to the image converter to streak it.

This method was necessitated by the irreproducibility in the discharge, because of variation in the gas pressure, gas composition (due to electrode material contamination), and bank voltage. Triggering on the  $dI/dt$  pulse which is picked up by a Rogowski coil at the back plate was tried but proved too unreliable.

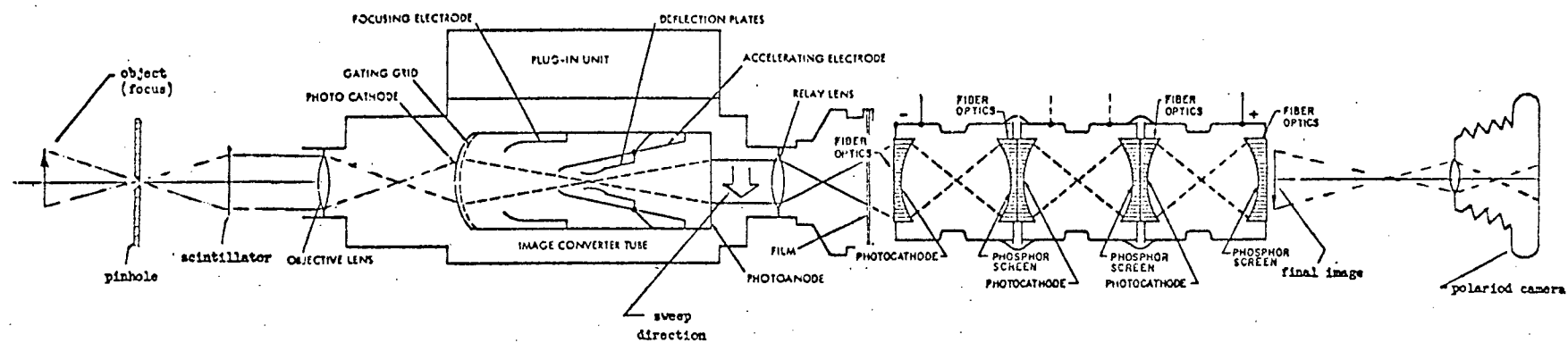


Figure 7. Electro-optical X-ray camera.

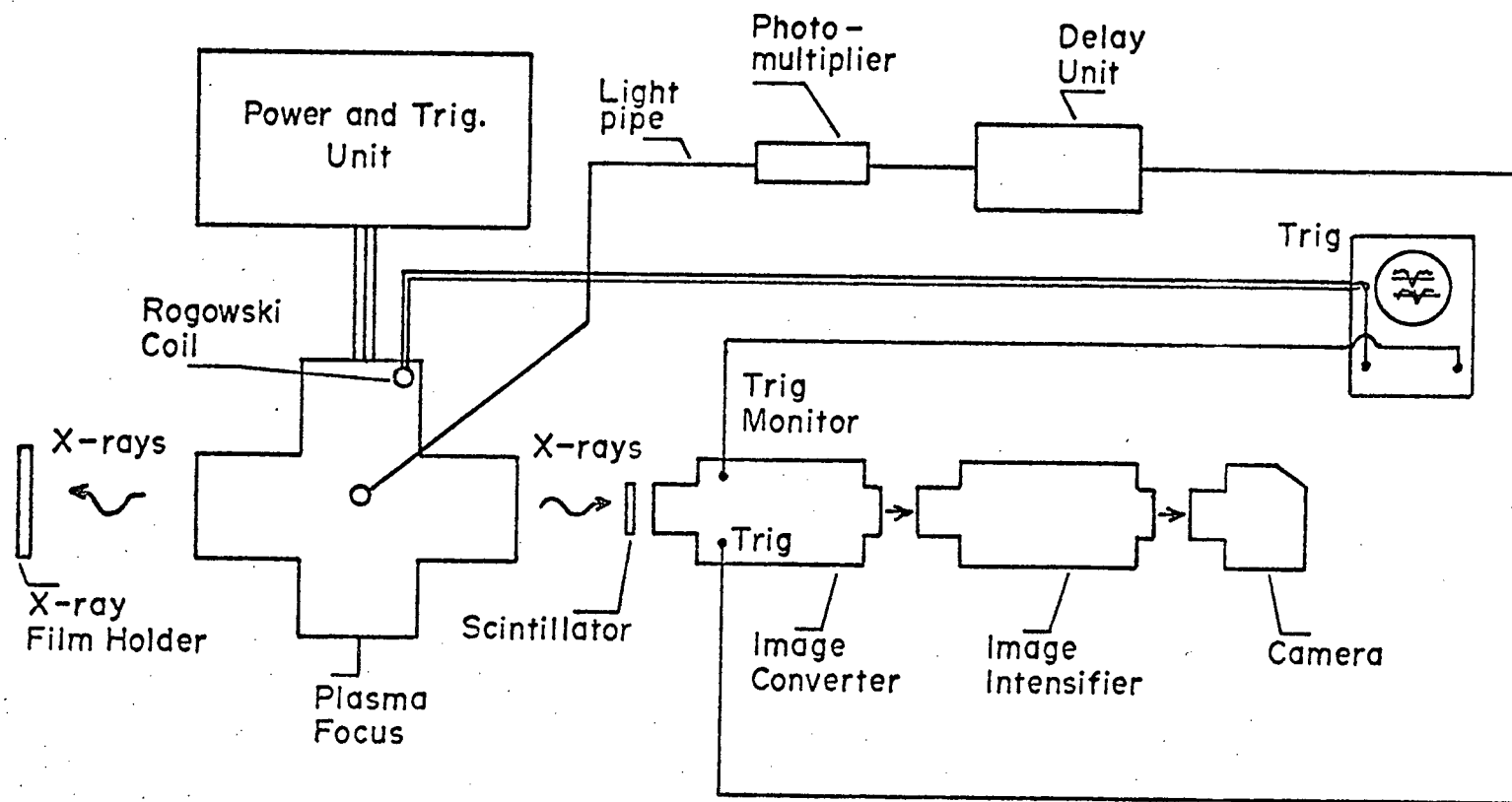


Figure 8. Triggering arrangement.



## Chapter 3

### OBSERVATIONS AND RESULTS

Before an interpretation of the X-ray photographs are made, measurements of the magnification, the streak speed, etc., must be done. The following describes how such measurements were conducted.

#### 3.1 Image Magnification

The magnification of the time integrated pictures was obtained by measuring the object-image distances from the focus to the pinhole and from the pinhole to the X-ray film, assuming that the object (i.e. the focus) is on the centre axis ( $z$ ) defined by the inner electrode. For the streak shot the object-image distances were measured to the scintillator. At the scintillator's surface two parallel white threads were used as objects in a separate experiment to determine the magnification between the scintillator and the film by measuring the real distance between the threads and that recorded by the film.

### 3.2 Spacial Resolution

The spacial resolution is limited to 1 mm and is determined by the pinhole diameter and optical geometry. The scintillator thickness (.15 cm) though affecting image formation does not affect the resolution due to the comparatively large distance (17 cm) between it and the pinhole.

The time duration of the streak from 50 to 200 nsec. was determined by the setting of the controls on the image converter unit. The length of the streak on the film was obtained by taking two pictures of the two parallel white threads, one at the beginning and one at the middle of the streak. This change in distance as recorded by the polaroid film, and the streak duration, determines the streak speed.

### 3.3 Temporal Resolution

The temporal resolution of the streak photographs is limited by the decay time of the plastic scintillator which is approximately 2 nsec. Since the image intensifier has a very long decay time (or after image) it had to be positioned after the streak unit or image converter in order that the temporal resolution was not sacrificed.

### 3.4 X-ray Photographs

Enlargements of the recorded X-ray pictures were taken such that the final enlargements of the time integrated

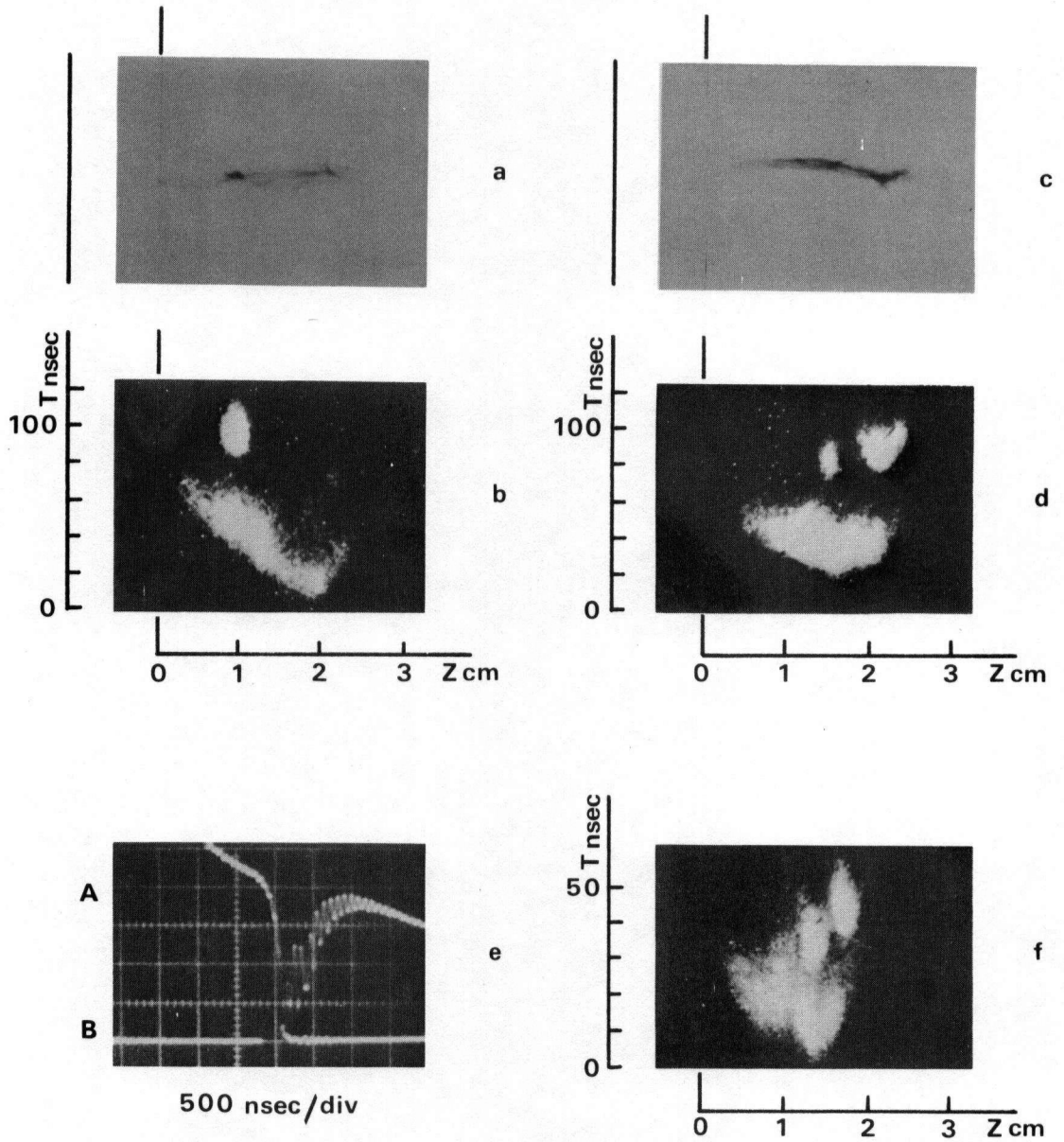
and streak shots have the same magnification (or ratio of image to object size).

These measurements combined with the photographs taken have given the following results and observations.

Two streak photographs with their corresponding time integrated X-ray photographs are shown in Fig. 9. From pictures as these it was determined that a long emitting X-ray region of plasma, extending over distances of order of centimeters with lifetimes of 30-60 nsec. is produced which moves axially towards and away from the anode at velocities between 2 and  $6 \times 10^7$  cm/sec.

This X-ray burst is followed 10-30 nsec. latter by small intense X-ray emitting regions extending over distances  $\leq .5$  cm with lifetimes of 10-30 nsec (see Fig. 9b,c). Some of these X-ray emitting regions exhibit no noticeable axial velocity (see Figure 9f). From spacial correlation with the corresponding time integrated photographs (see Fig. 9a,c) these sources show up as very small dark dots on the X-ray film in comparison to the softer and diffuse background produced from radiation emitted from an earlier time.

The  $dI/dt$  signal was displayed on a scope, the focus being indicated by a sudden dip in the  $dI/dt$  waveform (see oscillogram Figure 9e - upper trace A). The streak duration was also monitored and appears as a 'gap' in the lower trace (B), on the oscillogram. The real time of both traces coincide within 10 nsec. of each other, extrenous



(Z = axial distance from the electrodes)

Figure 9. X-ray photographs and an oscillogram of the focusing event.

time delay in the electrical cables and the equipment is taken into account when calculating this figure.

The discharging of the capacitors creates considerable electrical noise. This noise was eliminated by the use of ferrite cores on most of the electrical cables, and by the use of a light pipe for detecting the passage of the current sheath. To further minimize electrical interference the trigger delay unit, photomultiplier, and scope were placed in a shielded room. The room has double copper walls and the electrical power to this room was filtered before and after entering it.

## Chapter 4

### DISCUSSION OF RESULTS

The observed features of the focus agree well with the results of other experimenters who have studied the focus.

The time integrated photographs taken are similar to those obtained by Mather [10], Peacock [11], and Bostick [13].

Peacock [12] has observed that the sustainment time of the pinched plasma is not more than 50 nsec. and corresponds directly to the duration of the initial burst of thermal X-rays. He also found that the local break-up of the pinch is often due to  $m = 0$  instabilities, and that the time between formation of the dense pinch and its break-up is not greater than 100 nsec. These observations correspond well to the measured lifetimes of the heated (X-ray emitting) plasma as recorded by streak photography in this experiment.

Peacock [14] has further observed that the quasi-cylindrical compression produces a 'fountain' of a hot and dense plasma which travels axially away from the electrodes with a velocity of approximately  $10^7$  cm/sec., which agrees

with the measured observed radial velocities of  $2-6 \times 10^7$  cm/sec.

Bostick [13] observes that the duration of the X-ray emission from small individual intense sources is only 10 to 30 nsec. This agrees with observations in this experiment. But he incorrectly assumes that these small intense sources are triggered in *sequence* along the axial region. As is seen from the streak photograph 'f' in Fig. 4, this is clearly not always the case. Bostick states that  $10^7$  cm/sec. is the order of magnitude of the velocity of the plasma ejected from the axial region, which is in agreement with the values measured by Peacock and in this experiment.

From a time sequence of shadowgraphs Peacock observes that the dense pinch breaks up due to a  $m = 0$  instability and that the time interval between formation of the dense pinch and onset of the instability, the sustainment time, is of the order of 10 nsec. He measures further, that the wavelength of the instability, the distance between constrictions, is of the order of half a centimeter. From time resolved X-ray photographs of the plasma investigated here (see Fig. 4) one measures time intervals between the appearance of the X-ray emission, spreading over the whole pinch channel, and the appearance of the isolated point-like X-ray sources to be of the order of 10 nsec., which corresponds to Peacock's sustainment time. The distance between the

isolated X-ray sources is on the average half a centimeter which corresponds to the wavelength of the  $m = 0$  instability as observed by Peacock. These correlations strongly suggest that the appearance of the isolated X-ray sources is associated with the instability.

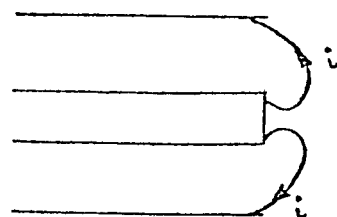
The features of the focus observed here and by Peacock suggest that the following sequences of physical events takes place. These events are describe in five stages.

The first stage is the collapse of the current sheath of the end of the electrodes, the  $B_0$  field compressing the gas mixutre rapidly inward. The second stage starts by the plasma being pinched, and as a result the plasma obtains an axial motion with velocities of the oder of  $10^7$  cm/sec. In the third stage the plasma cools by expansion and by radiative losses. Stage four starts when the instabilities, particularly the  $m = 0$  sausage instability forms, with growth rates of the order of 10 nsec., a time which is consistent with the observed times between the decay of the diffuse plasma and the creation of "hot" spots. As a result the plasma is heated by localized fields and X-ray emission occurs again. Since the pinch force or the magnetic  $B_0$  field is symmetric and perpendicular to the region of pinching, the plasma expands equally away and towards the electrode (with approximately the same axial velcoity) during its very short lifetime, and thus looks like an ablong 'dot' on the

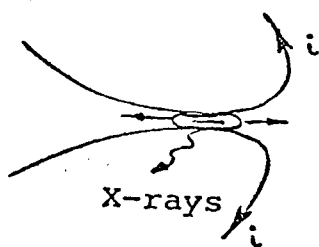


streak photograph. In stage five the "hot" spot in stage four continues to expand while at the same time rapidly cooling and emitting little or no X-rays.

This sequence would explain the observations during the formation and breakup of the dense focus stage as observed in this and other experiments. The following (Fig. 10) is a pictorial summary of the proposed process.



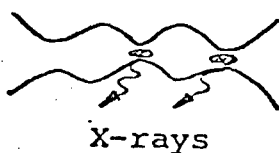
Stage 1



Stage 2



Stage 3



Stage 4



Stage 5

Stage 1 : gas is pinched by  $B_\theta$  field

Stage 2 : plasma is pinched, X-ray emission occurs

Stage 3 : plasma is cooling by expansion and radiative losses

Stage 4 :  $m=0$  instability forms, X-ray emission occurs

Stage 5 : Plasma expanding and cooling

Figure 10. Schematic for proposed sequence of events.

## Chapter 5

### CONCLUSIONS

Measurements of the X-ray emissions from the plasma focus by time integrated and streak photography has yielded information about the velocities, lifetimes and growth of the X-ray emitting regions.

A diffuse X-ray emitting plasma, extending several centimeters in the axial direction, having velocities of  $2-6 \times 10^7$  cm/sec. and lifetimes of 30-60 nsec. has been observed. This is followed 10-30 nsec. later by small intense X-ray sources which have little or no axial velocity, and lifetimes of the order of 10 nsec.

The distance between these short-lived small X-ray emitting regions correlated to observations made by Peacock strongly suggest that these X-ray sources are associated with the  $m = 0$  instability.

A possible model for explaining the sequence of X-ray events has been proposed which is consistent with the observations and measurements obtained by Peacock and Mather.

## REFERENCES

1. Mather, J.W., and Williams, A.H., Physics of Fluids, 9, 2081 (1966).
2. Mather, J.W., Nucleonics in aerospace - proceedings of the 2nd international symposium, Columbus, Ohio, U.S.A., 12-14 July 1967 (New York: Instrument Society of America 1968), pp. 290-6.
3. Pert, G.J., Brit. J. Appl. Physics, Ser. 2 Vol. 1, 1487 (1968).
4. Mather, J.W., Plasma Physics and Controlled Nuclear Fusion Research Vol. II, Proceedings of a Conference on Plasma Physics and Controlled Nuclear Fusion Research held by the I.A.E.A. at Culham, 6-10 Sept., 1965, pp. 389-403.
5. Toepfer, A.J., Smith D.R., and Becker, E.H., Physics of Fluids, Vol. 14, #1 (1971).
6. Peacock, N.J., *et al.*, 5th European Conference on Controlled Fusion and Plasma Physics, Grenoble, France, Vol. II, 21-25, Aug., 1972, p. 66.
7. Downing, J.N., The Physics of Fluids, Vol. 18, #8, 1975, pp. 991-1001.
8. Morgan, P.D., *et al.*, 3rd European Conference on Controlled Fusion and Plasma Physics, Novosibirsk, U.S.S.R., 1-7 Aug., 1968, p. 118.
9. Bernstein, M.J., and Hai, F., Physics Letters, Vol. 31A #6, 317 (1970).

10. Mather, J.W., The Physics of Fluids, Vol. 8, #2, 1965, pp. 366-377.
11. Long, J.W., Peacock, N.J., Wilcock, P.D., Topical Conference in Pulsed High Density Plasmas, Los Alamos, New Mexico, U.S.A., Sept. 19-22, 1967.
12. Peacock, N.J., Hobby, M.G., Morgan, P.D., 4th European Conference on Plasma Physics and Controlled Nuclear Fusion Research (International Atomic Energy Agency cn-28/D-3), Madison, Wisconsin, U.S.A., 17-23 June 1971, pp. 1-10.
13. Bostick, W.H., Nardi, V., Prior, W.J., and Rodriguez-Trelles, F., 5th European Conference on Controlled Fusion and Plasma Physics, Grenoble, France, Vol. II 21-25, August, 1972, p. 70.
14. Peacock, N.J., Wilcock, P.D., Speer, R.J., Morgan, P.D., 3rd European Conference on Plasma Physics and Controlled Nuclear Fusion Research (I.A.E.A. cn-24/G-4), Novosibirsk, U.S.S.R., 1-7 August, 1968, pp. 1-22.